# Coarsening mechanism of phase separation caused by a double temperature quench in an off-symmetric binary mixture

Tomoo Sigehuzi* and Hajime Tanaka†
*Institute of Industrial Science, University of Tokyo, Meguro-ku, Tokyo 153-8505, Japan*
(Received 6 June 2004; published 24 November 2004)

We study phase-separation behavior of an off-symmetric fluid mixture induced by a "double temperature quench." We first quench a system into the unstable region. After a large phase-separated structure is formed, we again quench the system more deeply and follow the pattern-evolution process. The second quench makes the domains formed by the first quench unstable and leads to double phase separation; that is, small droplets are formed inside the large domains created by the first quench. The complex coarsening behavior of this hierarchic structure having two characteristic length scales is studied in detail by using the digital image analysis. We find three distinct time regimes in the time evolution of the structure factor of the system. In the first regime, small droplets coarsen with time inside large domains. There a large domain containing small droplets in it can be regarded as an isolated system. Later, however, the coarsening of small droplets stops when they start to interact via diffusion with the large domain containing them. Finally, small droplets disappear due to the Lifshitz-Slyozov mechanism. Thus the observed behavior can be explained by the crossover of the nature of a large domain from the isolated to the open system; this is a direct consequence of the existence of the two characteristic length scales.

DOI: 10.1103/PhysRevE.70.051504 PACS number(s): 64.75.+g, 83.80.Tc, 64.60.Ht, 05.70.Fh

## I. INTRODUCTION

Phase separation is one of the most fundamental phenomena responsible for the formation of heterogeneous structures in condensed matter [1,2]. It is commonly observed in various kinds of condensed matter including metals, semiconductors, simple liquids, and complex fluids such as polymer solutions, colloidal suspensions, emulsions, and protein solutions. Generally, the dynamics and morphology of phase separation is strongly dependent upon the quenching conditions. From this standpoint, phase-separation phenomena are classified into nucleation-growth (NG)-type and spinodal-decomposition (SD)-type in the mean field picture [1,2]. Furthermore, SD-type phase separation is grouped into bicontinuous and droplet SD. So far most of studies on phase separation have been focused on the ordering process accompanied by a single rapid temperature quench from a one-phase to a two-phase region [1,2]. Kinetics of phase separation induced by a single temperature quench has reasonably been understood by intensive researches [3–7].

A quench condition including the composition and temperature of a mixture is one of the key factors that determine how the phase separation proceeds. There is a possibility that a variety of interesting phase-separated patterns are created by complex temperature modulations. One of such examples is periodic spinodal decomposition, which was theoretically predicted by Onuki [2,8] and experimentally studied by Joshua *et al.* [9] and also by us [10]. Effects of the thermal cycle on a gas-liquid transition was also investigated [11]. Here we focus our attention on the simplest multiple quench, namely, a double quench [12–14], which is composed of the first quench from a one-phase to a two-phase region and the second quench within the two-phase region. Although the final equilibrium state is determined solely by the final temperature, the process is strongly affected by the quench history. Thus, it is important to clarify how the quench history affects the kinetic pathway of phase separation. Here we consider this problem for a simple double temperature quench, where the second quench is a deeper one. Although the second quench can be a shallower one [14,15], we do not consider such a case in this paper.

The pattern evolution caused by this type of double quench has been studied experimentally and numerically by several groups [12–20]. In these studies, the structural evolution has been mainly analyzed in the wave-number ($q$) space. Here we aim at elucidating the characteristic feature of the pattern evolution induced by a double temperature quench by combining both *real* ($r$) and wave-number ($q$) space analyses. On the basis of these analyses, we propose a simple mechanism for domain coarsening of a hierarchic phase-separated structure.

The organization of this paper is as follows. In Sec. II, we describe the details of the experiments. In Sec. III, we describe the process of double phase separation induced by a double temperature quench. In Sec. VI, we analyze the patterns produced by double phase separation and their temporal change quantitatively. In Sec. V, we discuss the coarsening mechanism of double phase separation. In Sec. VI, we summarize our paper.

## II. EXPERIMENT

Samples used were binary mixtures of $\epsilon$-caprolactone oligomer (OCL) and styrene oligomer (OS). The OCL had the

*Present address: Nanotechnology Research Institute, National Institute of Industrials Science and Technology (AIST), Umezono 1-1-4, Tsukuba, Ibaraki, 305-8568, Japan.
†Corresponding author. Email address: tanaka@iis.u-tokyo.ac.jp

 

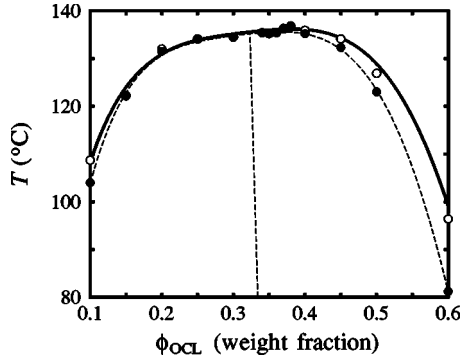


FIG. 1. The phase diagram of the OS/OCL mixture. The solid and dashed curves are the binodal and spinodal lines, respectively. The dashed line is the composition symmetry line.

weight-averaged molecular weight $M_w$ of 2000 and its ratio of the weight-averaged to the number-averaged molecular weight $M_w/M_n$ was 1.20. For the OS, $M_w=1000$ and $M_w/M_n=1.04$. The samples were sandwiched between the two cover glasses and the sample thickness was $\sim 3$ $\mu$m. We measured the binodal and spinodal temperatures of this system in various compositions by direct observation with phase contrast microscopy and determined the phase diagram with an upper critical solution temperature (UCST), as shown in Fig. 1. The sample temperature was controlled with a resolution of 0.1 K by a temperature-controlled hot stage (Linkam TH-600 RMS). The maximum rate of the temperature change was 1.5 °C/s.

We analyzed the structural evolution, which was observed with phase contrast microscopy, by using the digital image analysis (DIA) method [21]. For example, the structure factor $S(q)$ can be obtained by calculating the power spectrum of an image with the help of fast Fourier transformation (FFT). We use the zero-filling method to avoid the effect of leakage. We add the 20 areas with a value of zero about one direction around the original image, setting the average of the background level of the original image to zero. Then, the 2D-FFT of the whole image is processed. We also apply the smoothing operation for the 2D power spectrum to obtain a smooth structure factor. This operation is particularly useful for a small image, whose size is only several to ten times larger than the periodicity of the structure.

Various analyses in real space can also be made. This is a great advantage of DIA over the conventional scattering techniques.

## III. PHASE-SEPARATION BEHAVIOR AFTER A DOUBLE QUENCH

### A. Pattern evolution

First we describe the overall features of pattern evolution after a double temperature quench by demonstrating a typical example.

At the time $t=0$ we quench a OCL/OS(30/70) mixture from the stable to the unstable region ($T=T_1=132$ °C). After this first quench, spinodal decomposition takes place. In the late stage, droplets of the minority phase (the OCL-rich phase) are formed and coarsen with time. We call this structure formed by the first quench *the first-order structure*.

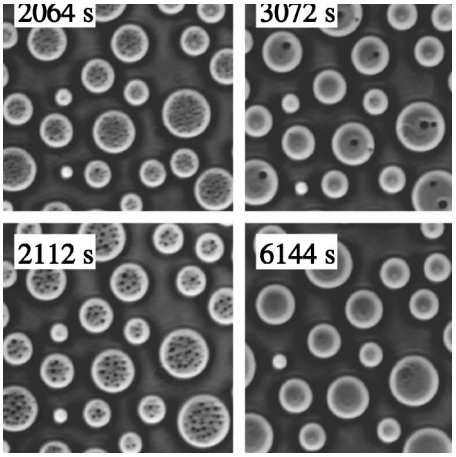


FIG. 2. Pattern evolution of the system after a double quench. [OCL 2000/OS 1000 (30/70), $T$:132 °C→130 °C→130 °C, $t_0$ =2048 s]. The second quench induces the phase separation of each phase. The phase with a dark contrast is the OS-rich one. The small droplets formed in the dark OCL-rich matrix phase disappear very quickly due to the wetting effects since they favor the glass walls and thus are very difficult to be observed. The secondary OS-rich droplets formed in the OCL-rich droplets, on the other hand, can be clearly seen since they are almost free from wetting effects [22].

Then, we applied the second quench to the system at $t=t_0=2048$ s; the temperature was further changed to $T_2=130$ °C. The pattern evolution of the system after this second quench is shown in Fig. 2. The time evolution inside a large OCL-rich droplet after the second quench can be seen in Fig. 3.

After the second quench there appeared small OS-rich droplets in the OCL-rich droplets formed by the first quench. We call this structure inside large droplets the *second-order structure*. First this subsystem coarsens with time mainly by the Brownian-coagulation mechanism [23–25] accompanying direct droplet collisions and coalescence. However, the

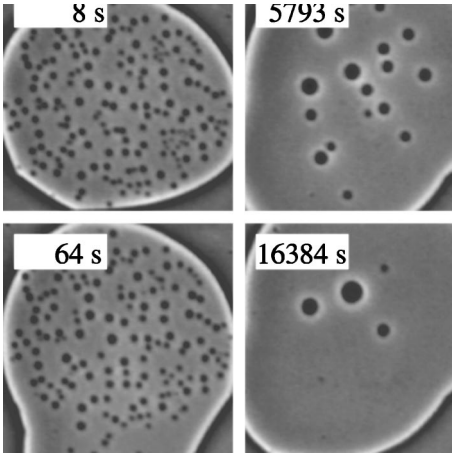


FIG. 3. Temporal change of the pattern inside a large OCL-rich droplet after the second quench. The size of an image corresponds to $25\times 25$ $\mu$m.

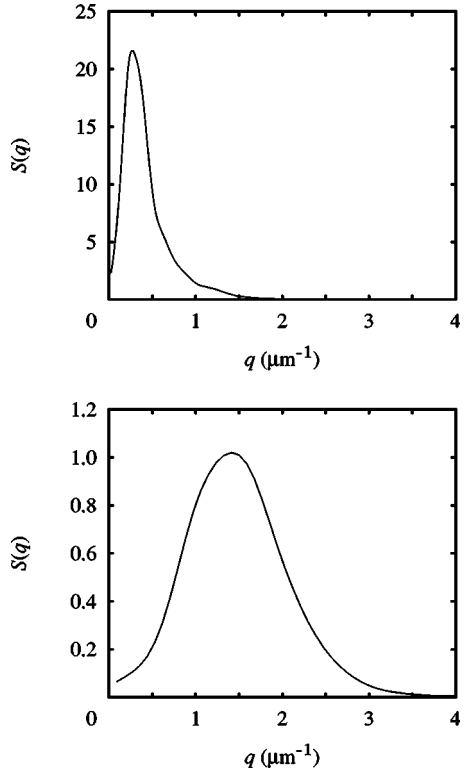


FIG. 4. Structure factor of the whole system (top) and the second-order structure only (bottom).

small droplets near the interface of the large OCL-rich droplet starts to *evaporate* and disappear. Eventually all the small OS-rich droplets disappear. This disappearance of the smaller droplets is controlled by the Lifshitz-Slyozov mechanism [23,26], as will be discussed later in detail. The qualitative feature is the same as that reported by one of the authors (H.T.) previously [14]. In the following section, we make quantitative analyses by using DIA.

### B. Wetting effects on pattern evolution

Since OCL is more wettable to glass than OS, phase separation is affected by wetting phenomena in a particular manner characteristic of this configuration [22]. It is worth mentioning that wetting effects can be strongly delocalized by hydrodynamic effects for fluid mixtures [22] and thus they do seriously affect phase-separation behavior even for a macroscopic sample. In relation to this, it is one of the advantages of *r*-space observation over *q*-space one that we can directly see how wetting effects affect the overall coarsening behavior. In our study, for example, we focus on the coarsening process of the second-order structure (small OS-rich droplets). This is because the coarsening behavior of small OS-rich droplets, which are less wettable to glass than the matrix phase, is not affected by wetting effects [22] (see also below). Since it is not the aim of this paper to study the wetting effects on phase separation and furthermore we are mainly interested in the effects of the second quench on pattern evolution, we do not dwell into the problem of wetting effects in this paper.

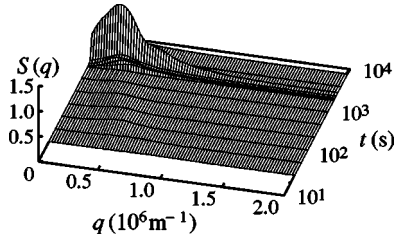


FIG. 5. Temporal change in $S(q)$ obtained by DIA. A system is OCL/OS(31/69). The mixture is quenched from the homogeneous state to the unstable state ($T_1$=130 °C) at $t$=0 and again quenched into the lower temperature ($T_2$=125 °C) at $t=t_0$=1800 s. When the peak intensity of $S(q)$ becomes maximum just after the second quench, we can clearly see the shoulder, which reflects the spatial correlation of small second-order droplets.

### C. Characteristics of *q*-space and *r*-space analyses of patterns using DIA

DIA is a very powerful method [21] to study the pattern evolution after a double quench. After the second quench a substructure is formed inside each droplet created by the first quench. Light scattering experiments provide the structure factor of the entire structure in the scattering volume. The structure factor $S(q)$ calculated from the patterns observed with phase-contrast microscopy, is essentially the same as that obtained by light scattering [21]. The top figure of Fig. 4 shows such a structure factor calculated by using DIA. This structure factor contains information on both large and small droplet structures, which give rise to the two scattering peaks. The small shoulder in $S(q)$ in the top figure of Fig. 4 reflects the spatial distribution of small droplets. However, the peak from the larger structure is much stronger than the one from the smaller structure and furthermore the separation of the two peaks is not so large. These facts make it difficult to obtain the precise information on the secondary (small) droplets, or the second-order structure, from the overall structure factor in light scattering experiments, although useful physical information can be extracted by careful analyses, as demonstrated by Hashimoto and co-workers [17,18].

In the case of DIA, on the other hand, a subimage that contains only the second-order structure can easily be obtained just by cutting an image. By applying the Fourier transformation to the subimage, a local structure factor can be calculated (see the bottom figure of Fig. 4). So the tem-

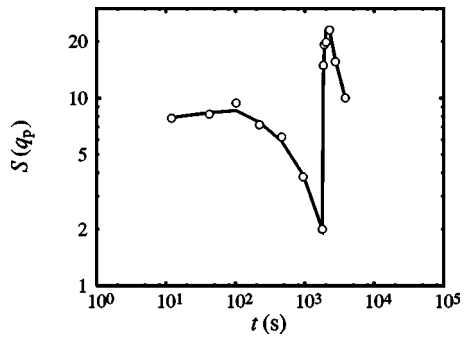


FIG. 6. Temporal change in the peak intensity $S(q_p)$ of the structure factor. $S(q_p)$ abruptly increases just after the second quench.

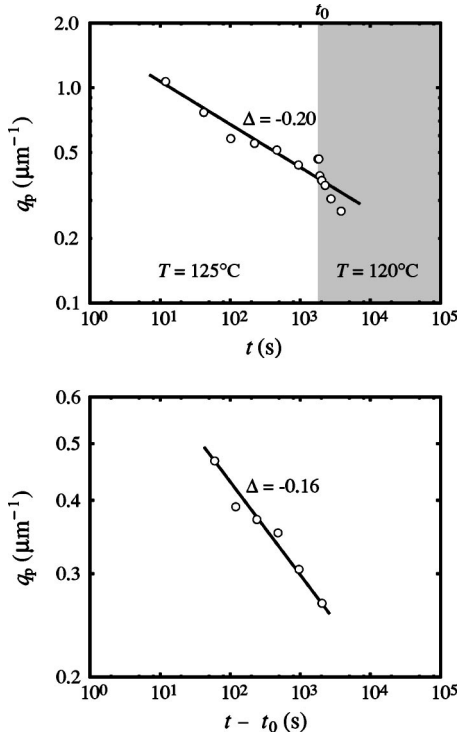


FIG. 7. Temporal change in the peak wave number $q_p$ of the DIA structure factor for the first-order structure (top). In the bottom figure, $q_p$ is plotted against $t-t_0$ instead of $t$. $\Delta$ is the exponent of the power law; $q_p \propto t^{\Delta}$.

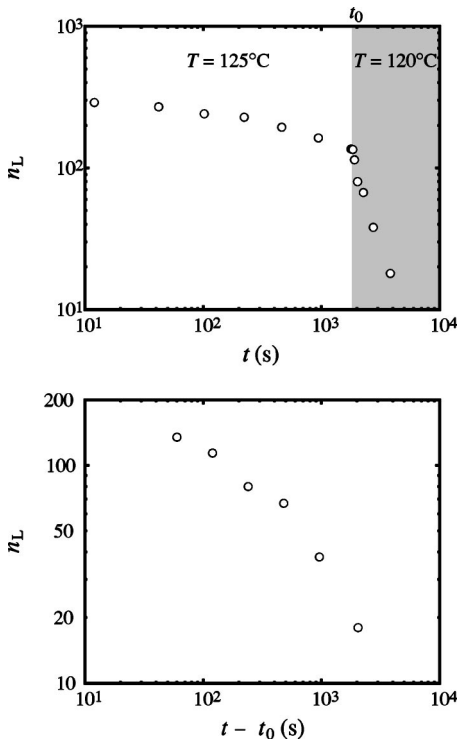


FIG. 8. Top figure: Temporal change in the number of the first-order droplets. Bottom figure: It is plotted against $t-t_0$ instead of $t$.

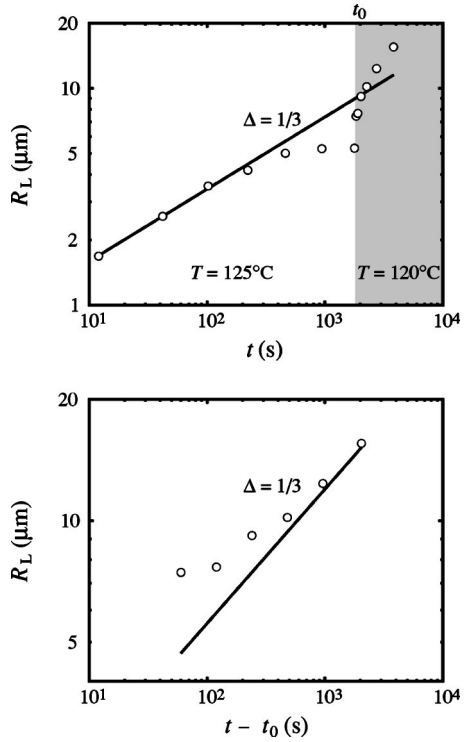


FIG. 9. Top figure: Temporal change in the number-averaged radius of the first-order droplets. Bottom figure: It is plotted against $t-t_0$ instead of $t$.

poral change of the second-order structure formed by the second quench inside the first-order structure (large droplets) can precisely be analyzed using DIA, as will be shown below.

Similarly, we can apply various $r$-space analyses to either the first-order or the second-order structure.

## IV. QUANTITATIVE ANALYSIS OF PHASE-SEPARATION PATTERNS INDUCED BY DOUBLE QUENCH

Here we analyze the pattern evolution induced by a double quench in detail by using DIA. As a typical example, we analyze phase separation of OCL/OS(31/69), which is quenched from the homogeneous state to the unstable state ($T_1$=130 °C) at $t$=0 and again quenched into the lower temperature ($T_2$=125 °C) at $t=t_0$=1800 s.

### A. Coarsening of the first-order structure

#### *1. q-space analysis*

In Fig. 5 we show the time evolution of the structure factor $S(q)$ of the first-order structure. The peak intensity of $S(q)$ decreases before the second quench, but it abruptly increases by the second quench, as shown in Fig. 6.

Figure 7 (top) shows the temporal change in the peak wave number of the structure factor corresponding to the first-order structure. After the first quench $q_p$ decreases, reflecting the coarsening of the first-order structure. The temporal change of $q_p$ is described by the power law $q_p \propto t^{\Delta}$ ($\Delta$ =−0.20 in this case). After the second quenched at $t=t_0$, the

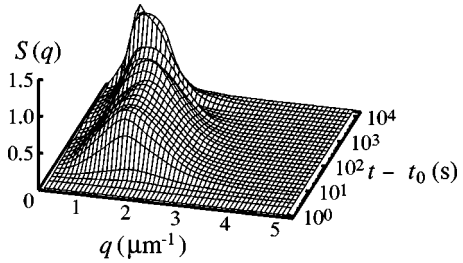


FIG. 10. Temporal change in the structure factor of the second-order structure alone.

coarsening rate is accelerated. The time dependence of $q_p$ no longer obeys the power law there. However, if we replot it against $t-t_0$ instead of $t$, we recover a power law [17,18] but with a different exponent ($\Delta=-0.16$) as shown in Fig. 7 (bottom). Since the coarsening is accelerated after the second quench, the memory of the system evolution up to time $t_0$ is soon lost.

#### *2. r-space analysis*

Here we describe the results of the real-space analysis of the pattern evolution. Figures 8 and 9 show the temporal changes of the number and the number-averaged radius of the first-order droplets, respectively. Since the process of the coarsening of the first-order (OCL-rich) droplets is affected by the wetting effects, no distinct scaling laws are observed. For example, the flow from the wetting layers to droplets bridging them apparently violates the in-plane conservation law [27,22]; this leads to the violation of the simple scaling law for the late-stage coarsening.

### B. Evolution of the second-order structure

Next we examine the temporal change of the second-order structure in detail.

#### *1. q-space analysis*

In Fig. 10 we show the time evolution of the local structure factor of the second-order structure. From this we can extract the temporal changes in the peak wave number and peak intensity, which are shown in Fig. 11.

Evidently there exist three time regimes for the time evolution of the local structure factor (see Fig. 11). In regime I,

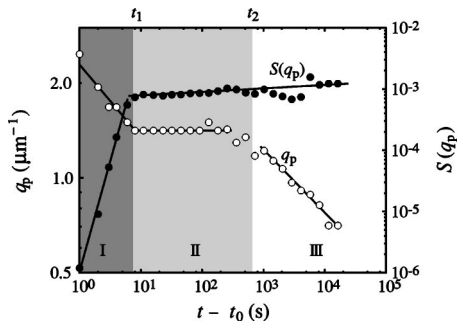


FIG. 11. Temporal change in the peak wave number $q_p$ (○) and the peak intensity $S(q_p)$ (●) of the local structure factor.

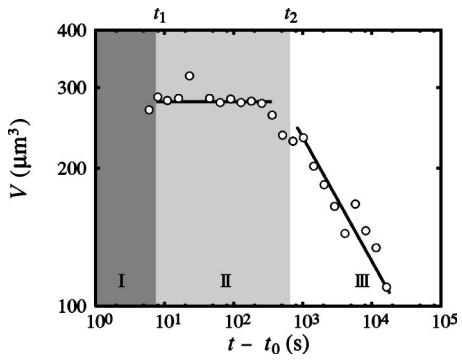


FIG. 12. Temporal change in the total volume of the OS-rich phase inside a first-order droplet, whose area is 9390 $\mu m^2$.

the peak wave number $q_p$ decreases with time, while the peak intensity $S(q_p)$ increases. In regime II, which starts at $t=t_1$, this tendency stops and both $q_p$ and $S(q_p)$ are almost constant with time. Finally, in regime III, which starts at $t=t_2$, $q_p$ starts to decrease again while $S(q_p)$ keeps stagnating [it finally decays (not shown), reflecting the disappearance of small droplets]. The coarsening of the second-order droplet is much slower than that of usual droplet phase separation induced by a single quench. This regime III continues until the second-order structure completely disappears.

#### *2. r-space analysis*

Next we show the results of the real-space analysis of the second-order structure. Figure 12 shows the temporal change in the total volume $V$ of the OS-rich phase (the phase making up the second-order droplets) in a first-order droplet (more precisely, in an area, which almost covers a particular first-order droplet and amounts to 9390 $\mu m^2$). In regimes I and II, $V$ is constant with time, while in regime III $V$ decreases with time obeying a power law. We also analyzed the temporal change in the number of the second-order droplets $n_S$ in the same first-order droplet as well as that in their number-averaged radius $R_S$; the results are shown in Figs. 13 and 14. The growth rate of the second-order droplets is much slower than usual phase separation, as mentioned above. $n_S$ decreases with time, while $R_S$ increases with time. For both cases, the rate of the change increases with time.

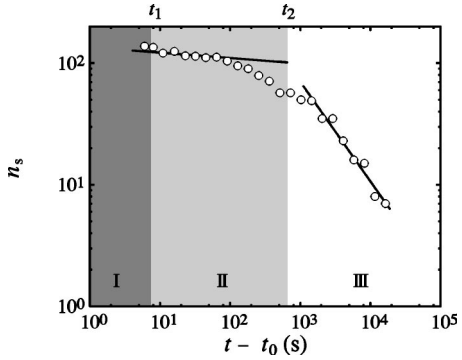


FIG. 13. Temporal change in the number of the OS-rich small droplets in the first-order droplet, whose area is 9390 $\mu m^2$. The slope of the solid line for regime III is −1.

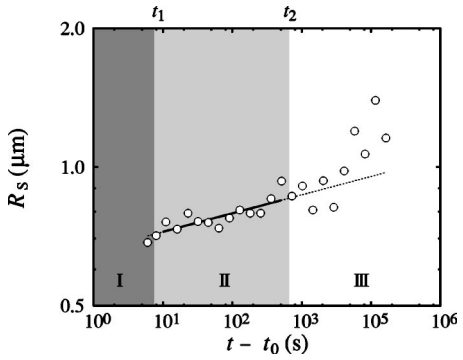


FIG. 14. Temporal change in the number-averaged radius of the OS-rich small droplets inside the first-order droplet. The growth of the droplet size is quite slow.

## V. DISCUSSION

Here we discuss the mechanism of the pattern evolution after a double quench on the basis of the above results. Let us consider the meaning of the key timings separating three regimes I–III. First we consider the meaning of the time $t_1$. There are two coarsening mechanisms in the late stage of droplet phase separation. One is the Brownian-coagulation mechanism and the other is the evaporation-condensation (Lifshitz-Slyozov) one [1,2,23]. Both processes give the same power law $q_p \propto t^{-\alpha}$ ($\alpha=1/3$ for three dimensions) [1,2,4,6,23,25]; in real space, $R^3=k_d(k_BT/5\pi\eta)t$, where $\eta$ is the viscosity and $k_B$ is the Boltzmann constant. For fluid mixtures both mechanisms are operative. Although the exponent is the same for both mechanisms, there is a crucial difference in the prefactor $k_d$ between them: the prefactor of the Brownian-coagulation mechanism is proportional to the volume fraction of the minority phase $\Phi_V$ ($k_d=6\Phi_V$), while that of the evaporation-condensation one only weakly depends upon it ($k_d \sim 0.053$). The prefactor becomes comparable when $\Phi_V$ is around 1%. We note that the volume fraction of the minority phase in the first-order droplet, which is estimated from $V$ (see Fig. 12), is just around this value.

Soon after the second quench (in regime I), the dominant coarsening mechanism is the Brownian-coagulation one, which we confirmed by the direct observation of the collision and coalescence process. At time $t_1$, however, the dominant coarsening mechanism switches from the Brownian-coagulation to the evaporation-condensation one. The above crossover was directly confirmed by microscopic observation of the elementary process of the droplet coarsening. Since the droplet size is too small in regime II, here we show in Fig. 15 a typical elementary coarsening process of the second-order small droplets due to the evaporation-condensation mechanism, which was observed in regime III. Note that it takes about $10^3$ s for the evaporation of the small droplet. Because of this slow coarsening kinetics of the evapolation-condensation process, the domain coarsening apparently looks as if it completely stops at $t_1$. Although the exact mechanism of this crossover and the difference in the coarsening speed are not clear at this moment, we speculate that this crossover behavior is induced by the rapid decrease in the droplet number density and/or the dimensional crossover from three to quasi two dimensions due to the finite thickness effect. Further theoretical studies are necessary to clarify the physical mechanism of the switching of the relevant coarsening mechanism.

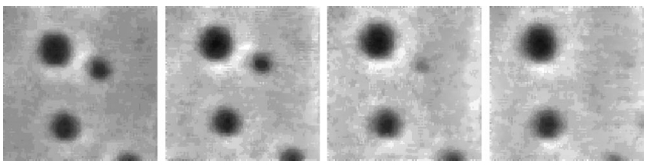

FIG. 15. The elementary process of domain coarsening due to the evaporation-condensation mechanism observed in a first-order droplet in regime III. The images correspond to $t-t_0=1448$, 1722, 2048, and 2436 s, respectively. The image size corresponds to $5 \times 5$ $\mu$m.

Next we consider the meaning of $t_2$. From the fact that the total volume of the secondary droplets starts to decrease from the time $t_2$ (see Fig. 12), we can conclude that $t_2$ is the time when the second-order system starts to lose the OS component due to its flux toward the interface of the large droplet; after $t_2$, the conserved nature of the coarsening behavior inside the first-order droplet starts to be violated "locally."

To understand this phenomenon, it is important to recognize the special situation of the intradroplet subsystem. The Lifshitz-Slyozov process arises from the fact that the smaller a droplet is, the higher the concentration of the component that is rich in the droplet phase at the matrix-side boundary of the droplet is. It should be noted [14] that the interface of the first-order droplet should be regarded as the boundary with a negative curvature for small secondary droplets. So the concentration near the inner boundary of the first-order OCL-rich droplet, $\phi_L$, should be lower than the final equilibrium value of the OCL-rich phase, $\phi_0$.

The Gibbs-Thomson relation [2] tells us that the concentration just inside the interface of the large OCL-rich droplet, $\phi_L$, is given by

$$\phi_L = \phi_0 - \Delta\phi \frac{2d_0}{R_L}, \tag{1}$$

where $R_L$ is the radius of the first-order droplet and $\Delta\phi$ is the concentration difference in the coexisting phases. Here $d_0$ is the so-called capillary length, which is give by [2]

$$d_0 = \frac{\sigma\xi^2}{2k_BT\Delta\phi^2}, \tag{2}$$

where $\sigma$ is the interface tension and $\xi$ is the correlation length, or the interface thickness. On the other hand, the concentration just outside a small secondary droplet of radius $R_S$ is given by

$$\phi_S = \phi_0 + \Delta\phi \frac{2d_0}{R_S}. \tag{3}$$

Equations (1) and (2) immediately tell us that $\phi_S > \phi_L$. This suggests that OS component, which is rich in the second-order droplets, is transferred via diffusion to the outside matrix OS-rich phase. Accordingly, the second-order droplets

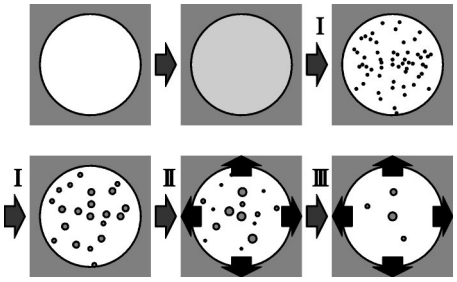


FIG. 16. Schematic figure describing the pattern evolution after a double quench. The thick black arrow indicates the diffusion flux induced by the concentration gradient.

evaporate and eventually disappear completely.

However, it takes some time for this diffusion process to be really operative. $t_2$, which separates regime II and III, can be regarded as the time required for the Lifshitz-Slyozov mechanism to be operative in the inner region of the large OCL-rich droplets. It is the characteristic diffusion time over the size of the large droplet and estimated as

$$t_2 \sim R_L^2/D_c. \tag{4}$$

Here $D_c$ is the mutual diffusion constant given by [2]

$$D_c = \frac{k_B T}{6\pi\eta\xi}. \tag{5}$$

Let us estimate the value of $t_2$. According to the mean-field theory

$$\xi = b\sqrt{\frac{\frac{1}{\phi}+\frac{1}{1-\phi}}{12\left(\frac{1}{N_A\phi}+\frac{1}{N_B(1-\phi)}-2\chi\right)}}, \tag{6}$$

where $b$ is the bond length, $N_A$ and $N_B$ are the degrees of polymerization of the two components, and $\chi$ is the interaction parameter. Here we use the relation $\chi \propto T_0/T$ ($T_0$ is a constant temperature); $T_0$ is determined as $T_0=22$ K from the critical temperature of our system. We also assume that the viscosity of the system is the simple weighted average of those of its components. The viscosities of OCL and OS were measured using a rotational viscometer, from which we got $\eta=0.090$ Pas. With these values and $N_A=106$, $N_B=18.5$, $b=0.153$ nm, and $T=125$ °C, we obtain $D_c=5.7\times10^{-12}$ m$^2$/s from Eqs. (5) and (6). By using $R_L=60$ $\mu$m, we estimate $t_2$ as $t_2=630$ s from Eq. (4). This is very much consistent with the experimentally determined value of $t_2 \sim 650$ s.

Here we summarize the physical scenario of the pattern evolution of the second-order structure (see Fig. 16). The second quench brings the intradroplet system into the unstable region and causes its spinodal decomposition into the two phases. When the process enters into the late stage of second spinodal decomposition, the Brownian-coagulation mechanism becomes the dominant coarsening mechanism (regime I). This mechanism keeps operative until the number density of the small droplets becomes too small for it to work. Then the dominant coarsening mechanism switches from the Brownian-coagulation mechanism to the evaporation-condensation one. This can be explained as follows. Both mechanisms are operative for fluid mixtures. However, since the latter depends on the droplet density less significantly than the former, the latter becomes more dominant than the former in the late stage, reflecting the decrease of the droplet density with time. This switching of the mechanism causes the drastic slowing down of the droplet coarsening (regime II). During regimes I and II, a subsystem can be regarded as an isolated system. However, this is no longer true in regime III and a subsystem (or a small droplet) starts to fully interact with the outer matrix phase. In other words, in regimes I and II small secondary droplets does not feel the concentration at the inner boundary of the first-order droplet, but at time $t_2$ they start to feel it and all small secondary droplets start to evaporate in regime III, since they evaporate and condensate onto the matrix phase surrounding the first-order droplet.

Finally, we point out that the characteristic times $t_1$ and $t_2$ are dependent upon the domain size of the first-order droplet $R$. Thus, the domain-size distribution that intrinsically exists in the first-order structure makes the crossover behaviors obscure, even though the individual domain has its unique and distinct crossover behavior. This is another merit of DIA analysis over the scattering techniques in revealing the physical mechanism.

## VI. CONCLUSION

In this paper we study the late stage of the phase-separation behavior of a binary mixture after a double quench using DIA method. We clarify the physical mechanism governing the complex phase-separation behavior. In particular, the secondary phase separation caused by the second quench can be separated into three characteristic regimes. In the first two regimes, a subsystem inside a large first-order droplet can be regarded as an isolated system, while in the last regime it can no longer be regarded as an isolated one and it strongly interacts with the surrounding matrix. This peculiar coarsening behavior is a direct consequence of the existence of the two characteristic length scales for double phase separation.

The phase-separation phenomena under a multiple quench is quite rich and interesting from both fundamental and applications viewpoints. For example, a multiple quench can transiently induce a hierarchic phase-separation structure. We also note that double phase separation can be induced even by a single quench [28] when the diffusion cannot catch up with the fast hydrodynamic coarsening. Further studies are highly desirable for clarifying the mechanism dominating hierarchical phase ordering under various multiple quenches and applying the phenomena to the structural control of material.

## ACKNOWLEDGMENT

This work was partly supported by a Grand-in-Aid for Scientific Research from the Ministry of Education, Culture, Sports, Science and Technology, Japan.

[1] J. D. Gunton, M. San Miguel, and P. Sahni, in *Phase Transition and Critical Phenomena*, edited by C. Domb and J. H. Lebowitz (Academic, London, 1983), Vol. 8.
[2] A. Onuki, *Phase Transition Dynamics* (Cambridge University Press, Cambridge, England, 2002).
[3] Y. C. Chou and W. I. Goldburg, Phys. Rev. A **20**, 2105 (1979).
[4] N. C. Wong and C. M. Knobler, Phys. Rev. A **24**, 3205 (1981).
[5] T. Hashimoto, M. Itakura, and N. Shimazu, J. Chem. Phys. **85**, 6118 (1986); T. Hashimoto, M. Itakura, and H. Hasegawa, *ibid.* **85**, 6773 (1986).
[6] P. Guenoun, R. Gastaud, F. Perrot, and D. Beysens, Phys. Rev. A **36**, 4876 (1987); F. Perrot, P. Guenoun, T. Baumberger, D. Beysens, Y. Garrabos, and B. LeNeindre, Phys. Rev. Lett. **73**, 688 (1994); P. Guenoun, D. Beysens, F. Perrot, Y. Garrabos, and A. Kumar, J. Phys.: Condens. Matter **6**, A199 (1994).
[7] F. S. Bates and P. Wiltzius, J. Chem. Phys. **91**, 3258 (1989).
[8] A. Onuki, Phys. Rev. Lett. **48**, 753 (1982).
[9] M. Joshua, W. I. Goldburg, and A. Onuki, Phys. Rev. Lett. **54**, 1175 (1985).
[10] H. Tanaka and T. Sigehuzi, Phys. Rev. Lett. **75**, 874 (1995).
[11] P. Guenoun, B. Khalil, D. Beysens, Y. Garrabos, F. Kammoun, B. LeNeindre, and B. Zappoli, Phys. Rev. E **47**, 1531 (1993).
[12] N. C. Wong and C. M. Knobler, J. Chem. Phys. **69**, 725 (1978).
[13] M. Okada, K. D. Kwak, and T. Nose, Polym. J. (Tokyo, Jpn.) **24**, 215 (1992).
[14] H. Tanaka, Phys. Rev. E **47**, 2946 (1993).
[15] M. Graca, S. A. Wieczorek, and R. Holyst, Macromolecules **35**, 7718 (2002); M. Fialkowski and R. Holyst, J. Chem. Phys. **117**, 1886 (2002).
[16] J. Tao, M. Okada, T. Nose, and T. Chiba, Polymer **36**, 3909 (1995).
[17] T. Hashimoto, M. Hayashi, and H. Jinnai, J. Chem. Phys. **112**, 6886 (2000).
[18] M. Hayashi, H. Jinnai, and T. Hashimoto, J. Chem. Phys. **112**, 6897 (2000).
[19] M. Rullmann and I. Alig, J. Chem. Phys. **120**, 7801 (2004).
[20] I. C. Henderson and N. Clarke, Macromolecules **37**, 1952 (2004).
[21] H. Tanaka, T. Hayashi, and T. Nishi, J. Appl. Phys. **59**, 3627 (1986); **65**, 4480 (1989).
[22] H. Tanaka, Phys. Rev. Lett. **70**, 2770 (1993); Europhys. Lett. **24**, 665 (1993); J. Phys.: Condens. Matter **13**, 4637 (2001).
[23] E. D. Siggia, Phys. Rev. A **20**, 595 (1979).
[24] H. Tanaka, Phys. Rev. Lett. **72**, 1702 (1994).
[25] H. Tanaka, J. Chem. Phys. **105**, 10099 (1996).
[26] I. M. Lifshitz and V. V. Slyozov, Phys. Chem. Solids **19**, 35 (1961).
[27] Note that we cannot observe the OCL-rich wetting layers by microscopic observation from the direction perpendicular to the glass walls.
[28] H. Tanaka, Phys. Rev. Lett. **72**, 3690 (1994); Phys. Rev. E **51**, 1313 (1995); H. Tanaka and T. Araki, Phys. Rev. Lett. **81**, 389 (1998).